View metadata, citation and similar papers at core.ac.uk
brought to you by CORE
provided by univOAK

Eur. Phys. J. Appl. Phys. **53**, 20501 (2011)
DOI: 10.1051/epjap/2010100364

THE EUROPEAN PHYSICAL JOURNAL APPLIED PHYSICS

Regular Article

# Fluorine-doped ZnO thin films deposited by spray pyrolysis technique

A. Douayar[1], R. Diaz[2], F. Cherkaoui El Moursli[3], G. Schmerber[4], A. Dinia[4], and M. Abd-Lefdil[1,a]

[1] Laboratoire de Physique des Matériaux, Faculté des Sciences, Rabat, Morocco
[2] Departamento de Física Aplicada C-XII, Universidad Autónoma de Madrid, Spain
[3] Équipe Batteries Lithium et Dépôts Électrolytiques, Faculté des Sciences, Rabat, Morocco
[4] Institut de Physique et Chimie des Matériaux de Strasbourg (IPCMS), UMR 7504 CNRS-UDS, 23 rue du Loess, BP 43, 67034 Strasbourg Cedex 2, France

Received: 22 September 2010 / Accepted: 5 November 2010
Published online: 28 January 2011 – © EDP Sciences

**Abstract.** Fluorine doped ZnO thin films (FZO) are prepared onto glass substrates at 350 °C by the chemical spray pyrolysis technique. X-ray diffraction spectra show a polycrystalline of ZnO (wurtzite structure) where the amount of fluorine doping affects to preferential orientation (002 plane along *c*-axis) and does not vary the lattice parameters. Therefore, F introduction in lattice is by the substitution of $O^{-2}$ ions by $F^{-1}$ ions. Any variation is observed in transmittance and reflectance measurements in 400–2000 nm wavelength range when samples present F dopant; they have transmittance around 80% in the near infrared and visible zones. The FZO films are degenerate and exhibit *n*-type electrical conductivity. The best resistivity and mobility are $7.6 \times 10^{-3}$ Ω cm and 3.77 $cm^2\ V^{-1}\ s^{-1}$ respectively. The calculated values of the mean free path are very small compared to the grain sizes calculated using XRD measurements. Therefore, we suggest that ionized impurity and/or neutral impurity scattering are the dominant scattering mechanisms in these films.

## 1 Introduction

Zinc oxide thin films have been investigated due to their important applications, e.g. as transparent electrodes and windows in solar cells [1–3], in gas sensors [4], and as converter of photons when it is doped with rare earths for third generation photovoltaic solar cells [5]. ZnO properties are strongly function of the crystalline structure, the nature and the amount of the used dopant. Most of the studies on doped ZnO thin films were carried out using divalent and trivalent cation dopants. However, a few studies on fluorine doped ZnO (FZO) can be found in the literature despite the fact that fluorine can be an adequate anion doping candidate due to its similar ionic radius to the oxygen. Thin films of ZFO can be prepared by many techniques, such as chemical vapor deposition [6], sputtering [7], sol-gel [8] and spray pyrolysis [9]. Among these techniques, spray pyrolysis is the most convenient method because of its simpleness, low cost, easy to add doping materials and the possibility of varying the film properties by changing composition of starting solution. This method is promising for high rate and mass production capability of uniform large area coatings in industrial applications.

In this work, a study of structural, electrical and optical properties is investigated in FZO thin films prepared by the chemical spray pyrolysis technique at 350 °C which is lower than used temperature in literature.

## 2 Experimental

Fluorine doped ZnO thin films were deposited on glass substrate by spray pyrolysis technique. An homogeneous solution is prepared by dissolving zinc chloride ($ZnCl_2$) [0.05 M] and ammonium fluoride ($NH_4F$) in distilled water at room temperature. Different solutions are prepared with different F content (in the 0–15 at.% F molar ratio range). Some drops of acetic acid ($CH_3COOH$) are added stirring 30 min at room temperature in order to avoid the precipitation of the solution. The glass substrate is cleaned in ethanol, rinsed in distilled water, and subsequently dried. All films are deposited at 350 °C during 77 min with a flow rate of the solution fixed at 2.6 mL/min. X′Pert Pro diffractometer is used to determine the X-Ray Diffraction (XRD) patterns with Cu $K_\alpha$ radiation. The surface morphology of the films is investigated using scanning electron microscopy (SEM) SEI Quanta 200. Transmittance and reflectance of films are measured in 400–2000 nm in a spectrophotometer (Cary 17D). Electrical properties are measured at room temperature using an ECOPIA Hall Effect Measurement System.

[a] e-mail: a-lefdil@fsr.ac.ma

## 3 Results and discussion

Figure 1 shows X-ray diffraction patterns of the several FZO thin films with different F concentration in solution. All samples present a polycrystalline single phase; all peaks corresponds to ZnO thin film, wurtzite structure, but peak intensity is different depending of the amount F dopant. The lattice parameters $a$ and $c$ do not vary with dopant percent of F in solution, $a$ = 3.23–3.25 Å and $c$ = 5.18–5.20 Å. The lattice size does not vary with F introduction indicating that the $F^{-1}$ ion is substitutive of $O^{-2}$ ion in the lattice, both ions present similar size. But the amount of dopant changes the preferential orientation in the thin film growth. In order to study these changes, an analysis of the peak intensities has be done from the study of texture coefficient $TCs$ $(hkl)$, associated to the texture of a particular plane [10]:

$$TC(hkl) = \frac{I(hkl)/I_0(hkl)}{(1/n)\sum_n I(hkl)/I_0(hkl)}; \quad (1)$$

Where $I(hkl)$ and $I_0(hkl)$ are the measured relative intensity of a plane $(hkl)$ and standard intensity of the plane $(hkl)$ taken from JCPDS data [card No. 80-0075] respectively, $n$ is the number of diffraction peaks.

Undoped ZnO and ZnO doped with high F concentration present very different TC coefficients of (002) and (101) planes; they decrease and increase between 2.25 to 1.78 and 0.85 to 1.34 respectively (Tab. 1). Therefore, undoped films has a preferential orientation along the (002) direction while high doped samples has this one along (101) plane.

Grain size of each sample is computed using the Scherrer's formula in (002) direction [11]:

$$D = \frac{0.9\lambda}{B\cos\theta}; \quad (2)$$

Where $\theta$ is the Bragg's diffraction angle of (002) plane, $B$ is the broadening of diffraction line at half its maximum intensity and $\lambda$ the wavelength of X-rays. Grain size was around 30 nm and it does not vary with the dopant content.

Figure 2 shows SEM images obtained for different FZO thin films. For undoped ZnO, the surface shows hexagonal grains with a grain size of 200–580 nm (Fig. 2a). Low F content (<5%at. ratio) in the sample produces a decrease of grain size (Fig. 2b). Samples with high F content (>10%at. ratio) present surface very different, likerod grains of different lengths (300–700 nm), which are composed of smaller rounded grains of various dimensions (Fig. 2c). This grain size, which corresponds to the grain size parallel to the substrate, are higher than the value computed from X-ray diffraction indicating that these grains are formed by several crystals.

The transmittance and reflectance spectra of FZO thin films are given in the 400–2000 nm wavelength range (Fig. 3). All the films exhibit a high transmittance between 75% and 85% in the visible range. A program permit to compute optical properties of thin films like absorption coefficient and film thickness considering multiple reflexion,

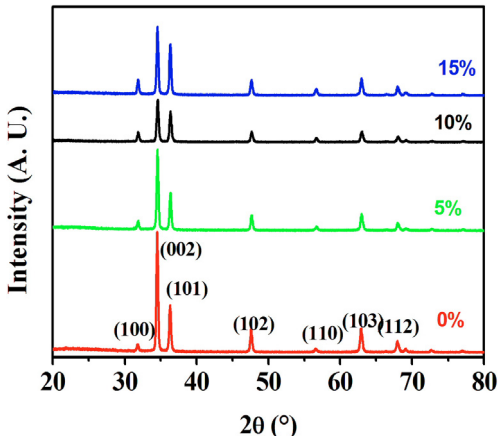


**Fig. 1.** (Color online) XRD patterns of FZO sprayed thin films.

**Table 1.** Various structural parameters of FZO sprayed thin films.

| F doping | $TC$ | | Crystallite | Lattice constant (Å) | |
|---|---|---|---|---|---|
| (at.%) | (002) | (101) | size, (nm) | $a$ | $c$ |
| 0 | 2.25 | 0.85 | 33 | 3.25 | 5.20 |
| 5 | 2.17 | 1 | 34 | 3.23 | 5.18 |
| 10 | 1.78 | 1.30 | 30 | 3.25 | 5.18 |
| 15 | 1.81 | 1.34 | 34 | 3.23 | 5.18 |

coherent and incoherent in the film and the substrate respectively. Figure 4 shows absorption spectra in the measured wavelength range; one can see that doped samples do not vary the optical properties respect to undoped sample. The plots of $(\alpha h\nu)^2$ versus $(h\nu)$ for the various F doped ZnO samples (Fig. 4), and the extrapolation of the linear portion of the plots onto the energy axis gives the band gap value around 3.18 eV.

For doped transparent conducting oxide films like FZO, carriers originate from intrinsic donors by lattice defects and/or extrinsic doping. In our case, the intrinsic donors are oxygen vacancies, and $Zn^{2+}$ atoms, and the extrinsic doping is the substitution of $F^-$ for $O^{2-}$ in ZnO lattice. Free electrons will be produced for every $F^-$ substitution, which will contribute to the electric conduction of the films as free carriers. All FZO thin films are $n$-type conducting, indicating that the fluorine acts as a donor-type impurity. Hall mobility, carrier density and resistivity measured at room temperature in samples with different fluorine doping content are done in Table 2. The electrical resistivity decreases by one order of magnitude when we pass from the undoped to fluorine doped ZnO and presents a slight variation with increasing fluorine doping level. The minimum of electrical resistivity measured is $7.6 \times 10^{-3}$ Ω cm, obtained for 5% of F. It is in the same order of magnitude that other samples grow by other techniques (Tab. 3). One can also note for sprayed films that the thickness and the used temperature are lower than those reported in literature. The carrier density $n$ increases with fluorine doping varying in the $1.75 \times 10^{19}$–$54.91 \times 10^{19}$ $cm^{-3}$ range. The mobility $\mu$ decreases and

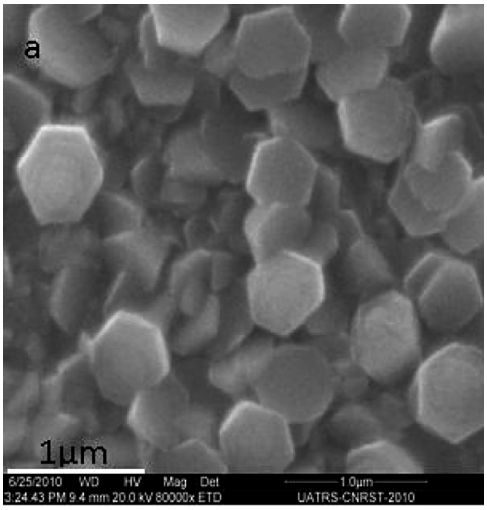


(a)

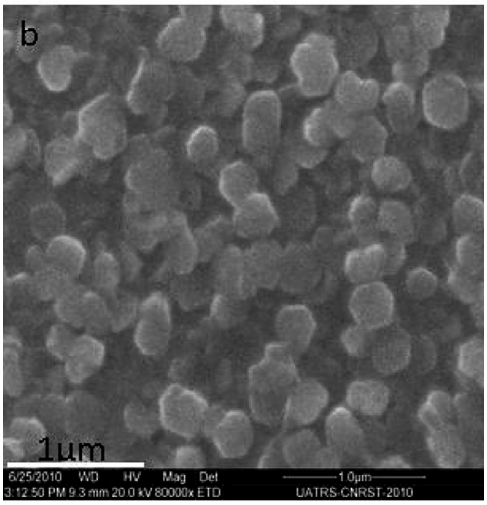


(b)

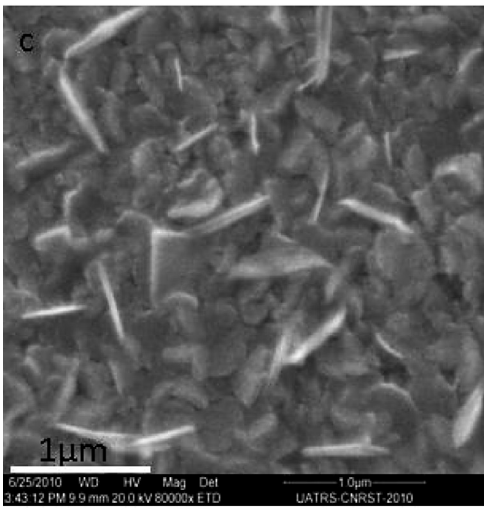


(c)

**Fig. 2.** SEM images of FZO sprayed thin films. (a) ZnO: 0% F, (b) ZnO: 5% F and (c) ZnO: 10% F.

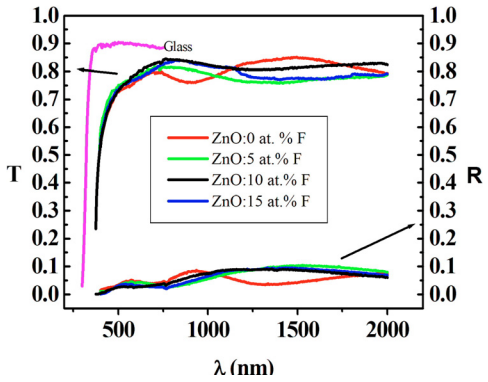


**Fig. 3.** (Color online) Transmittance and reflectance spectra FZO sprayed thin films.

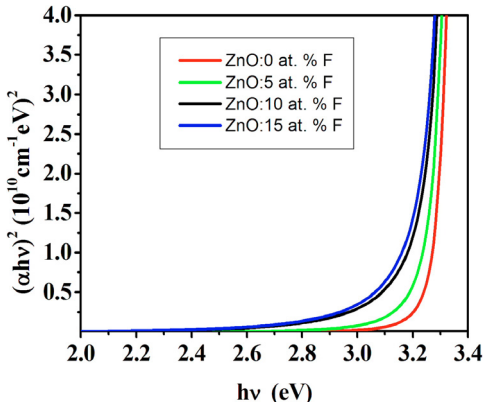


**Fig. 4.** (Color online) $(\alpha h\upsilon)^2$ versus $h\upsilon$ for FZO sprayed thin films.

it is lower than those obtained on sputtered films [7,12]. A low mobility can be explained by the interaction between the carriers and the scattering mechanisms. These carrier scattering mechanisms include lattice vibration, dislocation, grain boundary, ionized impurity, and neutral impurity scattering. The degeneracy of our samples is confirmed by the evaluation of the Fermi energy level using the relation [13]:

$$E_F = \left(\frac{h^2}{8m^*}\right)\left(\frac{3n}{\pi}\right)^{2/3}; \quad (3)$$

Where $m^* = 0.3\ m_e$, $m_e$ is the electron rest mass and $n$ is the carrier concentration. The calculated $E_F$ values are higher than the energy corresponding to the room temperature (0.03 eV). As can be observed, the values of mobility decreases when the doping content increases The mean free path $\beta$ of the free carriers is calculated using [13]:

$$\beta = \left(\frac{h}{2e}\right)\left(\frac{3n}{\pi}\right)^{1/3}\mu; \quad (4)$$

Where, $h$ and $e$ are Plank's constant and electron charge respectively. $\beta$ values are shown in Table 2 and they are considerably smaller than the grain sizes calculated using XRD. Therefore, we suggest that ionized impurity and/or neutral impurity scattering are the dominant scattering mechanisms in these films [14].

**Table 2.** Various electrical parameters of FZO sprayed thin films.

| F doping (at.%) | Thickness (nm) | $\rho$ $10^{-3}$ ($\Omega$ cm) | $\mu$ cm$^2$ V$^{-1}$ s$^{-1}$ | $n$ $10^{19}$ cm$^{-3}$ | $\beta$ (nm) |
|---|---|---|---|---|---|
| 0 | 440 | 74.1 | 4.82 | 1.75 | 0.53 |
| 5 | 470 | 7.6 | 3.77 | 21.66 | 0.45 |
| 10 | 430 | 7.8 | 1.45 | 54.91 | 0.24 |
| 15 | 450 | 74.6 | 0.48 | 17.45 | 0.11 |

**Table 3.** Electrical resistivity of FZO sprayed thin films as reported by other authors and in the present study.

| | $\rho \times 10^{-3}$ ($\Omega$ cm) | Preparation technique | Thickness (nm) | Reference |
|---|---|---|---|---|
| FZO | 7.6 | Spray (350 °C, $NH_4F$) | 470 | This work |
| | 7.8 | Spray (500 °C, HF) | 600 | [9] |
| | 1.3 | Spray (450 °C, $NH_4F$) | 550 | [15] |
| | 8.6 | Spray (450 °C, $NH_4F$) | 700 | [17] |
| | 1.9 | Sputtering+ | – | [12] |
| | 3.6 | Sputtering+ | – | [7] |
| | 1000 | Sol-gel | – | [16] |
| | 0.4 | CVD | – | [6] |

For sprayed films (preparation temperature, source of fluorine) + with annealing treatment.

In order to summarize the properties of our TCO's, the figure of merit was calculated using Haacke's [18] equation: $F_{TC} = T^{10}/R$ where $T$ is the value of optical transmission at $\lambda = 550$ nm and $R$ is the sheet resistance given by $R = \frac{\rho}{d}$ where $d$ is the thickness of the film. For 5% of fluorine content, $R$ is around 163 $\Omega/$ and the $F_{TC}$ value is $4.5 \times 10^{-4}$ $\Omega^{-1}$ in a good agreement with recent works on TCOs [10,19,20].

## 4 Conclusion

Fluorine doped ZnO thin films (FZO) are prepared onto glass substrates by the chemical spray pyrolysis technique at 350 °C which is lower than used temperature in literature. The films are polycrystalline with a preferential orientation (002) plane along $c$-axis. This orientation is affected by fluorine doping and a switch from the (002) to the (101) orientation is reported. Transmittance around 80% in the visible zone is reported. The FZO films are degenerate and exhibit $n$-type electrical conductivity. The best obtained value of resistivity is $7.6 \times 10^{-3}$ $\Omega$cm for 5% fluorine content. The calculated values of the mean free path are very small compared to the grain sizes calculated using XRD, which can explain the lowest obtained mobility values. This suggest that ionized impurity and/or neutral impurity scattering are the dominant scattering mechanisms in these films. The above-mentioned characteristics render these FZO films potential candidates for their use as a window in solar cells and in optoelectronic devices, with the advantage that they are prepared by a simple and economical technique.

This work has been done in the framework of the Morocco-Hispano University Collaboration by the Spanish Agency of International Cooperation Project No. A/027536/09.

## References

1. A.V. Singh, R.M. Mehra, N. Buthrath, A. Wakahara, A. Yoshida, J. Appl. Phys. **90**, 5661 (2001)
2. X.P. Peng, J.Z. Xu, H. Zang, B.Y. Wang, Z.G. Wang, J. Lumin. **128**, 297 (2008)
3. J.B. Lee, H.J. Lee, S.H. Seo, J.S. Park, Thin Solid Films **641**, 398 (2001)
4. N. Hongsith, E. Wongrat, T. Kerdcharoen, S. Choopun, Sens. Actuat. B: Chem. **144**, 67 (2010)
5. T. Trupke, M.A. Green, P. Würfel, J. Appl. Phys. **92**, 1668 (2002)
6. H. Jianhua, R. Gordon, Sol. Cells **30**, 437 (1991)
7. H.S. Yoon, K.S. Lee, T.S. Lee, B. Cheong, D.K. Choi, D.H. Kim, W.M. Kim, Sol. Energy Mater. Sol. Cells **92**, 1366 (2008)
8. S. Ilican, Y. Caglar, M. Caglar, F. Yakuphanoglu, Appl. Surf. Sci. **255**, 2353 (2008)
9. J. Rodríguez-Báez, A. Maldonado, G. Torres-Delgado, R. Castanedo-Pérez, M. de la L. Olvera, Mater. Lett. **60**, 1594 (2006)
10. S.S. Shinde, P.S. Shinde, S.M. Pawar, A.V. Moholkar, C.H. Bhosale, K.Y. Rajpure, Solid State Sci. **10**, 1209 (2008)
11. P. Scherrer, Gottinger Nachrichten Gesell. **2**, 98 (1918)
12. Y.Z. Tsai, N.F. Wang, C.L. Tsai, Thin Solid Films **518**, 4955 (2010)
13. B. Thangaraju, Thin Solid Films **402**, 71 (2002)
14. M. Oshima, K. Yoshino, J. Electron. Mater. **39**, 819 (2010)
15. S.M. Rozati, S. Moradi, S. Golshahi, R. Martins, E. Fortunato, Thin Solid Films **518**, 1279 (2009)
16. D.C. Altamirano-Juiarez, G. Torres-Delgado, S. Jimienez-Sandoval, O. Jimienez-Sandoval, R. Castanedo-Pierez, Sol. Energy Mater. Sol. Cells **82**, 35 (2004)
17. B.N. Piwar, D.H. Ham, R.S. Mane, T. Ganech, B.W. Cho, S.H. Han, Appl. Surf. Sci. **254**, 6294 (2008)
18. G. Haacke, J. Appl. Phys. **47**, 4086 (1976)
19. H.J. Park, J.H. Park, J.I. Choi, J.Y. Lee, J.H. Chae, D. Kim, Vacuum **83**, 448 (2009)
20. M. Ait Aouaj, R. Diaz, A. Belayachi, F. Rueda, M. Abd-Lefdil, Mater. Res. Bull. **44**, 1458 (2009)